International Journal of Advanced Engineering Research and Science (IJAERS)
Peer-Reviewed Journal
ISSN: 2349-6495(P) | 2456-1908(O)
Vol-8, Issue-10; Oct, 2021
Journal Home Page Available: https://ijaers.com/
Article DOI: https://dx.doi.org/10.22161/ijaers.810.4

Signal Received Power Mapping in Wireless Communication Networks using Time Series and Geostatistics

Edilberto Rozal[1], Evaldo Pelaes[2]

[1]Department of Mathematics, Federal University of Pará (UFPA), Castanhal, Pará, Brazil
[2]Electrical Engineering Department, Federal University of Pará (UFPA), Belém, Pará, Brazil

Received: 01 Sep 2021,

Received in revised form: 25 Sep 2021,

Accepted: 04 Oct 2021,

Available online: 10 Oct 2021

***Keywords*—ARIMA Model, Geostatistics, Kriging, Multivariate Temporal Modeling, Wireless.**

***Abstract*—*Some theoretical and experimental models have been considered for the prediction of the path loss in mobile communications systems. However, one knows that in real environment, the received signal is subject to variations. The model developed for an urban area cannot give resulted acceptable for different urban areas since that, each model has different parameters in accordance with the considered area. This paper presents the results of propagation channel modeling, based on multivariate time series models using data collected in measurement campaigns and the main characteristics of urbanization in the city of Belem-PA. Transfer function models were used to evaluate effects on the time series of received signal strength (dBm) which was used as the response variable and as explanatory variables of the height of buildings and distances between buildings. As time series models disregard to the possible correlations between neighboring samples, we used a geostatistical model to establish the correctness of this model error. The results obtained with the proposed model showed a good performance compared to the measured signal, considering the data of the eleven routes from the center of the city of Belém/Pa. From the map of the spatial distribution of the received signal strength (dBm), one can easily identify areas below or above dimensional in terms of this variable, that is benefited or damaged compared with the signal reception, which may result in a greater investment of the local operator (concessionaire mobile phone) in those regions where the signal is weak.*

I. INTRODUCTION

Nowadays there is a great variety of communications channel models, with fundamental theories and experiments with a prediction on path loss in mobile communication systems. These models differ in their applicability, on different types of terrain and different environmental conditions. Thus, there is not an existing appropriate model for all situations. In real cases, the terrain on which the propagation presents varied topography, vegetation and constructions are randomly distributed. Although the propagation loss calculation can be performed, although with limited accuracy, using techniques such as ray tracing or numerical solutions for approximations of the wave equation.

The propagations models are generally based on the deterministic models (Liaskos et al., 2018; Salous, 2013; Shu Sun et al., 2014)[1-3] and modified based on results obtained from measurement campaigns in one or more

regions [2]. The models obtained are given by expressions that provide the median value of attenuation, like the models of Okumura-Hata(Arthur et al., 2019) [4]consisting analytical expressions of the average attenuation route, for urban areas, suburban and open (rural). These formulations are limited to certain ranges of input parameters, and are applicable only to land almost flat and are valid for frequencies of 150 to 1500 Mhz. and the model of Ibrahim-Parsons(Rozal et al., 2012) [5], which takes into account factors such as the degree of urbanization, land usage, and the variation in height between the mobile station (MS) and the base transceiver station (BTS). These empirical characteristics were extracted from measurements taken in the city of London, on frequencies between 168 and 900 MHz. This model was studied in urban areas without undulations. It is used for distances between antennas smaller than 10 km and receiving antenna height of less than 3 m.

The model of Walfisch–Ikegami(Alqudah, 2013) [6]has its formulation based on characteristics of urban regions, such as density and average height of buildings, and the width of the streets. This model is effective in cases where the height of the antennas BTS is smaller than the average height of buildings a situation where there is considerable guidance signal RF along the routes considered. This model predicts two different situations for calculating the average attenuation path between BTS and the mobile: The line of sight (LOS— line of sight and Non-line-of-sight (NLOS).

This paper presents a model for time series to characterize the received signal strength (dBm) in eleven pathways downtown of Belém/PA. The work consisted in the study of the possible relationship between this received signal strength and the behavior of the height of the buildings and the distance between. Transfer function models were used to assess effects on time series of the received strength and to evaluate the relationship between the height of the buildings and the distance between buildings.

For error correction model in time series, instead of using another ARIMA model, a spatial geostatistical model based on kriging was used. This module includes a set of required procedures for geostatistical techniques (exploratory analysis, generation and modeling of a semivariogram and kriging). With the objective an analysis in two dimensions for spatially distributed data, with respect to interpolation of surfaces generated from the geo-referenced samples obtained from the received strength.

II. RELATED WORKS

The literature analysis of propagation models has investigated different statistical prediction methods to identify appropriate techniques for thispurpose. Currently, many propagation channel models employ the most varied modeling techniques, such as time series modeling and geostatistics. In(Konak, 2010)[7] estimated signal propagation losses in wireless LANs using Ordinary Kriging (OK). In (Phillips et al., 2012) [8] used OK on a 2.5 GHz WiMax network to produce radio environment maps that are more accurate and informative than deterministic propagation models. In(Kolyaie et al., 2011)[9] used drive-tests to collect signal strength measurements and compared the performance of empirical and spatial interpolation techniques.(Y. Zhang et al., 2012)[10] developed a methodology based on time series analysis and geostatistics through experiments using a real dataset from the Swiss Alps. The results showed that the developed methodology accurately detected outliers in wireless sensor network (WSN) data, by taking advantage of their spatial and temporal correlations. Edilberto Rozal et al. [5] presented results of propagation channel modeling, based on multivariate time series models and the main characteristics of urbanization in the city of Belém/PA by using data collected in measurement campaigns. Transfer function models were used to evaluate the relationship between the received signal strength and other variables, such as building's height, distance between buildings, and distance to the radio base station, which were recorded in a street in the city center of Belém/PA, Brazil.(Karunathilake et al., 2014)[11] studied location-based systems to investigate the availability of signal reception levels, specifically 3G and 4G signals. The study was based on geostatistical analysis using the inverse distance weighting (IDW) method.(Molinari et al., 2015)[12] empirically studied the accuracy of a wide range of spatial interpolation techniques, including various forms of Kriging, in different scenarios that captured the unique characteristics of sparse and non-uniform measurements and measurements in imprecise locations. The results obtained indicated that ordinary Kriging was an overall fairly robust technique in all scenarios.(Wen-jing et al., 2017)[13] proposed a traffic prediction method based on the seasonal autoregressive integrated moving average (S-ARIMA) model, according to the characteristics of the network traffic and its respective implementation.(K. Zhang et al., 2019)[14] proposed a system for traffic analysis and prediction suitable for urban wireless communication networks, which combined actual call detail record (CDR) data analysis and multivariate prediction algorithms.(Mezhoud et al., 2020) [15]proposed an approach for coverage prediction based on the hybridization of the interpolation technique by OK and a Neural Network with MLP-NN architecture, this methodology was motivated by the lack of quality of the

MLP-NN test database, which satisfactorily enriched the network's training dataset.(Song et al., 2020)[16] used a novel secure data aggregation solution based on the ARIMA model to prevent tracking of private data by opponents.(Faruk et al., 2019)[17]evaluated and analyzed the efficiencies of empirical, heuristic and geospatial methods for predicting signal fading in the very high frequency (VHF) and ultra-high frequency (UHF) bands in typically urban environments. Path loss models based on artificial neural network (ANN), adaptive neuro-fuzzy inference system (ANFIS) and Kriging techniques were developed. Sato et al.(Sato et al., 2021)[18]proposed a technique that interpolates the representative map of the mobile radio signal in the spatial domain and in the frequency domain.

III. TIME SERIES

A time series is a set of statistics, usually collected at regular intervals.Time series data occur naturally in many application areas, such as economics, finance, environmental and medicine. The methods of time series analysis pre-date those for general stochastic processes and Markov Chains. The aims of time series analysis are to describe and summarize time series data, fit low-dimensional models, and make forecasts [5].

We write our real-valued series of observations as $\ldots X_{-2}, X_{-1}, X_0, X_1, X_2, \ldots$, a doubly infinite sequence of real-valued random variables indexed by integers numbers.

One simple method of describing a series is that of classical decomposition. The notion is that the series can be decomposed into four elements:

Trend (T_t) — long term movements in the mean;

Seasonal effects (I_t) — cyclical fluctuations related to the calendar;

Cycles (C_t) — other cyclical fluctuations (such as a business cycles);

Residuals (E_t) — other random or systematic fluctuations.

The idea is to create separate models for these four elements and then combine them, either additively:

$$X_t = T_t + I_t + C_t - E_t \quad (1)$$

or multiplicatively:

$$X_t = T_t . I_t . C_t . E_t \quad (2)$$

3.1. ARIMA Models

Box and Jenkins [5] first introduced ARIMA models, the term deriving from: AR = Autorregressive, I = Integrated and MA = Moving average.

A key concept underlying time series processes is that of stationarity. A time series is stationarity when it has the following three characteristics:

(a) Exhibits mean reversion in that it fluctuates around a constant long-run mean;

(b) Has a finite variance that is time-invariant;

(c) Has a theoretical correlogram that diminishes as the lag length increases.

The autoregressive process of order p is denoted AR(p), and defined by

$$Y_t = \sum_{i=1}^{p} \varphi_i Y_{t-i} + e_t \quad (3)$$

Where $\varphi_1,\ldots,\varphi_r$ are fixed constants. Y_t is expressed linearly in terms of current and previous values of a white noise series $\{e_t\}$. This noise series is constructed from the forecasting errors; $\{e_t\}$ is a sequence of independent (or uncor-related) random variables with mean 0 and variance σ^2.

Using the lag operator L (the lag operator L has the property: $(L^n Y_t = Y_{t-n})$ we can write the AR(p) model as:

$$Y_t(1 - \varphi_1 L - \varphi_2 L^2 - \ldots - \varphi_p L^p) = e_t \quad (4)$$

$$\Phi(L) Y_t = e_t \quad (5)$$

Where $\Phi(L)Y_t$is a polynomial function ofY_t.

The moving average process of order q is denoted MA(q) and defined by:

$$Y_t = e_t + \sum_{i=1}^{q} \theta_j e_{t-j} \quad (6)$$

Where,$\theta_1,\ldots, \theta_q$ are fixed constants, $\theta_0 = 1$, and $\{e_t\}$ is a sequence of independent (or uncorrelated) random variables with mean 0 and variance σ^2.

Or using the lag operator:

$$Y_t = (1 - \theta_1 L - \theta_2 L^2 - \ldots - \theta_p L^q) u_t \quad (7)$$

$$Y_t = \Theta(L) u_t \quad (8)$$

The combination of the two processes to give a new series of models called ARMA (p, q) models, is defined by

$$Y_t = \sum_{i=1}^{p} \varphi_i Y_{t-i} + e_t + \sum_{i=1}^{q} \theta_j e_{t-j} \quad (9)$$

Where again $\{e_t\}$ is white noise, $\{\varphi_i / i = 1,2,..,p\}$are the coefficients of AR model and $\theta_i / i = 1,2,..,q\}$ are the coefficients of MA model.

Using the lag operator:

$$Y_t(1 - \varphi_1 L - \varphi_2 L^2 - \ldots - \varphi_p L^p) = (1 - \theta_1 L - \theta_2 L^2 - \ldots - \theta_p L^q) \quad (10)$$

$$\Phi(L) Y_t = \Theta(L) e_t \quad (11)$$

According to the target model, the process is non-stationary, so the series should be transformed to a stationary process be the model construction. This can be

often achieved by a differentiation process.The first-order differencing of the original time series is defined as:

$$\Delta Y_t = Y_t - Y_{t-1} = Y_t - BY_t \qquad (12)$$

For the high-order differentiation, we have:

$$\Delta^d Y_t = (1-B)^d Y_t \qquad (13)$$

If we ever find that the differenced process is a stationary process, we can look for a ARMA model of that. The process $\{Y_t\}$ is said to be an autoregressive integrated moving average process, ARIMA(*p*,*d*,*q*). If $X_t = \Delta^d Y_t$ is an ARMA (*p*, *q*) process.

After the *d*-order differentiations of $Y_t$in equation 10, the autoregressive integrated moving average (ARIMA), ARIMA (*p*,*d*,*q*), can be constructed as:

$$\Phi(L) Y_t^d = \Theta(L) e_t \qquad (14)$$

A time series (TS) may be defined as a set of observations Y_t as a function of time [5]. The principal tools utilized for analysis of a time series are the autocorrelation and partial autocorrelation functions.

The autocorrelation function (ACF) represents a simple correlation between $Y_t$and Y_{t-k}as a function of the lag *k*. The autocorrelation function of TS $\{Y_t\}$ may be defined as: [5].

$$\rho = \frac{\sum_{t=0}^{N-k-1}(Y_t-\overline{Y})(Y_{t+k}-\overline{Y})}{\sum_{t=0}^{N-1}(Y_t-\overline{Y})^2} \qquad (15)$$

Where *N* represents the length of the TS and $\bar{Y}$is the expected value from the observations, calculated for the time variation (*delay*) *k*. The autocorrelation coefficient (ρ) of a TS varies between –1 and 1.

The partial autocorrelation function (PACF) represents the correlation between $Y_t$and Y_{t-k}as a function of the lag *k*, filtering the effect of the other lags on $Y_t$and Y_{t-k}. The partial autocorrelation function is defined as the sequence of correlations between (Y_t and Y_{t-1}), (Y_t and Y_{t-2}), (Y_t and Y_{t-3}) and so on, because the effects of prior lag on *t* remain constant. The PACF is calculated as the coefficient value φ_{kk} in the equation:

$$Y_t = \varphi_{k1} Y_{t-1} + \varphi_{k2} Y_{t-2} + \varphi_{k3} Y_{t-3} + \ldots + \varphi_{kk} Y_{t-k} + e_t \qquad (16)$$

3.2. Transfer Function Model

Transfer function model is different from ARIMA model. ARIMA model is univariate time series model, but transfer function is multivariate time series model. This means that ARIMA model relates the series only to its past. Besides the past series, transfer function model also relates the series to other time series. Transfer function models can be used to model single-output and multiple-output systems [5]. In the case of single-output model, only one equation is required to describe the system. It is referred to as a single-equation transfer function model. A multiple-output transfer function model is referred to as a multi-equation transfer function model or a simultaneous transfer function (STF) model [5].

Assume that $X_t$and Y_t are properly transformed series such that both are stationary. In a linear system with simple input and output, the series of X_t input and Y_t output are related through a linear filter as

$$Y_t = \nu(B) X_t + N_t \qquad (17)$$

Where $\nu(B) = \sum_{-\infty}^{\infty} \nu_j B^j$ is referred to as a filter transfer function by Box and Jenkins and N_t is a noise series of the system that is independent of the input series X_t

The coefficients in the transfer function model (17) are often called the impulse response weights.

The objective of modeling the transfer function is to identify and estimate the transfer function $\nu(B)$ and the noise model for $\boldsymbol{N_t}$ based on the information available for the input series X_t and the output series Y_t. The greatest difficulty is that information regarding $X_t$andY_t is finite, and the transfer function in (17) contains an infinite number of coefficients. To alleviate this difficulty, the transfer function $\nu(B)$ is shown in the following rational form: [5]

$$\nu(B) = \frac{w_s(B) B^b}{\delta_r(B)} \qquad (18)$$

Where$w_s(B) = W_0 - W_1 B - \ldots - W B^s$, $\delta_r(B) = 1 - \delta_1 B - \ldots - \delta_r B^r$, and b is a lag parameter that represents the delay that elapses before the impulse of the input variable produces an effect on the output variable. For a stable system, it is assumed that the roots of $\delta_r(B) = 0$ lie outside the unit circle [5]. After obtaining$w_s(B)$, $\delta_r(B)$ and b, the ν_j weights of the impulse response can be obtained by setting the coefficients of B^jon both sides of the equation equal to one another:

$$\delta_r(B)\, \nu(B) = w_s(B)\, B^b \qquad (19)$$

In practice, the values of *r* and *s* on the system (8) rarely exceed 2. Some transfer functions can be seen in [5]. These models may be used to identify the parameters of the transfer function. Analysis of these models show that the occurrence of peaks suggests parameters in the numerator of the transfer function, similar to models of moving averages, and the occurrence of an exponential decay behavior may indicate the existence of parameters in the denominator of the transfer function, similar to the autoregression models.

IV. GEOSTATISTICS

Geostatistics is used in the spatial interpolation and uncertainty quantification for variables that exhibit spatial continuity, i.e, can be measured at any point of the area / region / area under study. Using traditional statistical concepts as random variable (VA) cumulative distribution function (FDA), probability density function (PDF),expected value, variance, etc. These concepts can be found in statistical textbooks. In geostatistics, the VA, represented by $z(u)$, where u is the vector of coordinates of the location, is related to some location in space. In this case, the main statistics are set out below. The cumulative distribution function (FDA) gives the probability that the VA Z is less than or equal to a certain value z, generally called cutoff value(Chilès & Delfiner, 2012; Gooverts, 1984; Isaaks, 1990; Johnston et al., 2001; Pyrcz & Deutsch, 2014; Shiquan Sun et al., 2020; Tobler, 1989)[19-25]

4.1 Description of Spatial Patterns

In earth science is often important to know the pattern of dependence of one variable X over another Y. The joint distribution of results of a pair of random variables $X$and $Y$is characterized by the FDA joint (or bivariate) defined as:

$$F_{XY}(x,y) = prob\{X \le x;\ Y \le y\} \qquad (20)$$

estimated in practice the proportion of data pairs below the respective joint values (cutoff values) x and y. This can be shown in the scatter diagram (Fig. 1) in which each pair of data (x_i,y_i)is plotted as a point.

The degree of dependence between the two variables X and Y can be characterized by the dispersion around 45º in the scattergram. The great reliance ($X = Y$) matches all experimental pairs (x_i,y_i), i = 1,..., N plotted on the line 45º.

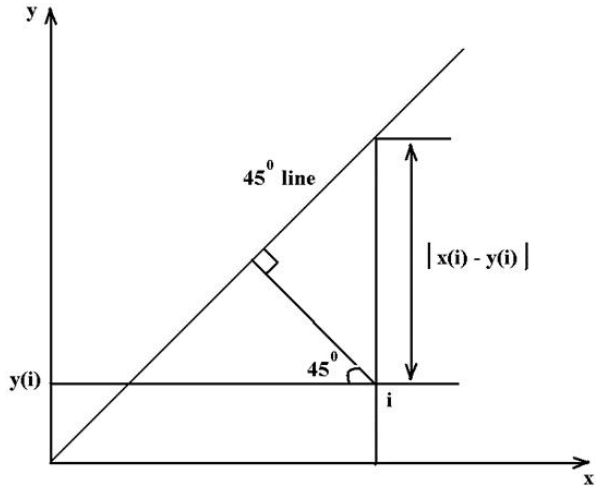

Fig. 1: Pair (x_i ,y_i) on a scattergram

The moment of inertia of the scattergram around the 45º line – called "semivariogram" for all pairs (x_i,y_i) – is defined as half the average of squared differences between the coordinates of each pair, i.e.:

$$\gamma_{XY} = \frac{1}{N}\sum_{i=1}^{N} d_i^2 = \frac{1}{2N}\sum_{i=1}^{N}(x_i - y_i)^2 \qquad (21)$$

The higher the value of the semivariogram, the greater dispersion and less closely related are the two variables X and Y.

In problems of spatial interpolation, where one want to infer (map) a certain area for a given property, $z(u), u \in$ area A, starting from a sample n of $z(u)$. The combination of all $n(h)$ pairs of data of$z(u)$, over the same area/zone/layer/population A with such pairs separated by approximately the same vector h (in length and direction), allows estimating the semivariogram characteristic (or experimental) of the spatial variability in A:

$$\gamma(h) = \frac{1}{2N(h)}\sum_{\alpha=1}^{N(h)}[z(u_\alpha) - z(u_\alpha + h)]^2 \qquad (22)$$

An experimental semivariogram (22) is an estimate of an integral discrete space defining a well determined on average$A$:

$$\gamma_A(h) = \frac{1}{A(h)}\int_A [z(u) - z(u+h)]^2\, du \quad \text{for } u,\ u+h \in A. \qquad (23)$$

Such as a VA $z(u)$ is and its distribution characterizes the uncertainty about the value of certain property located at u, a random function $z(u)$, $u \in A$, defined as a set of VA's dependent feature of joint spatial uncertainty about A. The semivariogram of this random function characterizes the degree of spatial dependence between two random variables $z(u)$ *and* $z(u+h)$ separated from the vector h.

For the modeling of the semivariogram conducted after building the experimental semivariogram, it is necessary that the hypothesis is considered stationary. This hypothesis states, in summary, that the first two moments (mean and variance) of the difference $[z(u) - z(u+h)]$ are independent of location u and function only for the vector h. The second moment of this difference corresponds to the semivariogram, i.e:

$$2\gamma(h) = E\{[z(u) - z(u+h)]^2\} \text{is independent to } u \in A. \qquad (24)$$

Developing the equation above (adding m^2 to all terms for convenience), one obtains:

$$2\gamma(h) = C(0) - C(h), \qquad (25)$$

and that:

$$Var\{Z(u)\} = Var\{Z(u+h) = \sigma^2 = C(0) \quad \text{for all} \quad u \in A. \qquad (26)$$

$Cov\{Z(u), \{Z(u+h) = C(h) \text{forall} u \in A$ (27)

The relation (25) is then utilized to determine the semivariographic model. The variance $C(0)$ is called in geostatistics a baseline (or sill). The semivariogram can be defined as the graph of the semivariance function versus distance$h$,is a technique used to measure the dependence between sample points, distributed according to a spatial reference and for interpolation of values required for the construction of isoline maps [19]. According to Christakos(Christakos, 1984)[26], is the preferred tool for statistical inference because it offers some advantages over the covariance, including:

i) Its empirical calculation is subject to minor errors;

ii) Provides a better characterization of the spatial variability;

iii) Requires the called intrinsic stationarity assumption, i.e. that $z(u)$ is a random function with stationary increments $z(u+h) - z(u)$, but not necessarily itself stationary.

The semivariogram is the preferred tool for statistical inference because it offers some advantages over the covariance [19]. For a continuous function is selected a semivariogram necessary to satisfy the property of positive definite. In practice are used linear combinations in basic models that are valid, i.e., permissible. One of the most used basic models in geostatistics is the spherical model, given
by:

$$\gamma_{(h)} \begin{cases} 0, & |h| = 0 \\ C\left[\frac{3}{2}\left(\frac{|h|}{a}\right) - \frac{1}{2}\left(\frac{|h|}{a}\right)^3\right] & 0 < |h| \leq a \\ C & |h| > a \end{cases} \quad (28)$$

The components C $anda$ are denominated the level and range, respectively. The level, also known as "sill" represents the variability of the semivariogram to its stabilization. The range (or variogram range) and the distance are observed up to the level where the variability stabilizes. Indicates the distance in which the samples are spatially correlated (Fig. 2).

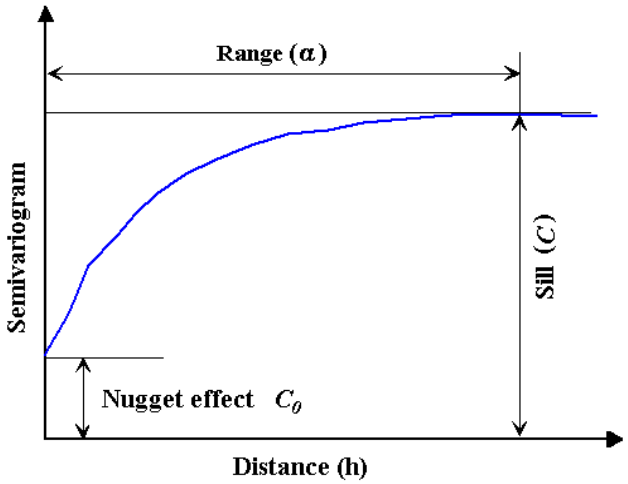

Fig. 2: Parameters of the semivariogram

4.3 Ordinary Kriging

Kriging is a interpolation technique in which the surrounding measured values are weighted to derive a predicted value for an unmeasured location. Weights are based on the distance between the measured points, the prediction locations, and the overall spatial arrangement among the measured points. Kriging is based on regionalized variable theory, which assumes that the spatial variation in the data being modeled is homogeneous across the surface. Ordinary Kriging (OK) considers the local variation of the mean limited to the domain of stationary of the average local neighborhood $W(u)$ centered on the location u to be estimated [24-25]. In this case, one considers the common average (stationary) $m(u)$ in equation 43, e.i.:

$$Z^*(u) = \sum_{\alpha=1}^{n(u)}[\lambda_\alpha(u) z(u_\alpha) + \left[1 - \sum_{\alpha=1}^{n(u)}[\lambda_\alpha(u)\right] m(u) \quad (29)$$

The mean $m(u)$ unknown can be eliminated by considering the sum of the weights$\lambda_\alpha(u)$ of kriging equal to 1. This mode:

$$Z^*_{KO*}(u) = \sum_{\alpha=1}^{n(u)}[\lambda_\alpha^{KO}(u) z(u_\alpha), \text{with} \quad \sum_{\alpha=1}^{n(u)}[\lambda_\alpha^{KO}(u) = 1 \quad (30)$$

The minimization of the error variance ($Var[Z^*(u) - Z(u)]$) under the condition $\sum_{\alpha=1}^{n(u)}[\lambda_\alpha^{KO}(u) = 1$, allows to determine the weights λ_α from the following system of equations called ordinary kriging system (normal equations with constraints):

$$\begin{cases} \sum_{\beta-1}^{n} \lambda_\beta^{KO}(u) C(u_\beta - u_\alpha) + \mu(u) = C(u - u_\alpha) \\ \sum_{\beta-1}^{n} \lambda_\beta^{KO}(u) = 1 \qquad\qquad \alpha = 1, \ldots . n \end{cases} \quad (31)$$

where $C(u_\beta - u_\alpha)$ and $C(u - u_\alpha)$ are, respectively, the covariance between the points $u_\beta$and u_α, u and $u_\alpha . \mu_u$is

the Lagrange parameter associated with the restriction: $\sum_{\beta-1}^{n} \lambda_{\beta}^{KO}(u) = 1$.

The kriging system (31) presents only one solution if:

i) The covariance function $C(h)$ is positive-definite, i.e.:

$$Var\{\sum_{\alpha=1}^{N} \lambda_{\alpha} z(u_{\alpha})\} = \sum_{\alpha=1}^{N} \sum_{\beta=1}^{N} \lambda_{\alpha}\lambda_{\beta} C(u_{\alpha} - u_{\beta}) \geq 0 \quad (32)$$

ii) There are not two completely redundant data, i.e, $u_{\alpha} \neq u_{\beta}$ if $\alpha \neq \beta$.

The corresponding minimum variance of the error, called the kriging variance is given by:

$$\sigma_{KO}^2 = Var[Z(u) - Z^*(u)] = C_0 - \sum_{\varepsilon=1}^{n(u)} \lambda_{\alpha} C(u_{\beta} - u_{\alpha}) - \mu(u) \quad (33)$$

where $C_0 = Var\{Z(u)\} = \sigma^2$.

Substituting the expression for its covariance $C(h) = C_0 - \gamma(h)$, the system (31) and the variance σ_{KO}^2 can be written as a function of the semivariographic model$\gamma(h)$.

Therefore, unlike the more traditional linear estimators, kriging uses a system of weights that considers a specific model of spatial correlation, variable to the area A under study. Kriging provides not only a least squares estimate of the variable being studied, but also the variance error associated(D. Istok & A. Rautman, 1996) [27].

V. MATERIALS AND METHODS

5.1 Database

A local telecommunications company provided technical characteristics of broadcast stations and the received signal of the routes described. This area is the urban center of Belém/PA. The acquisition of vertical and tested measures of the buildings and homes, totaling approximately 4500 points (between residents and buildings) was done by AUTOCADMAP and ORTOFOTO obtained with a plant scanned from**the Company for Metropolitan Development and Administration of Belém - CODEM.** Belém, capital of the state of Pará, belonging to the Metropolitan Mesoregion of Belém with an area of approximately 1 064,918 km², located in northern Brazil, with latitude -01° 27' 21" and longitude of -48° 30' 16", altitude of 10 meters and distance 2 146 Km of Brasília. Is known as "Metropolis of the Amazon", and one of the ten busiest and most attractive of Brazil. The city of Belem is considered the biggest of the equator line, is also classified as a capital with the best quality of life in Northern Brazil.Fig.3 shows the routes used in the measurement campaign.

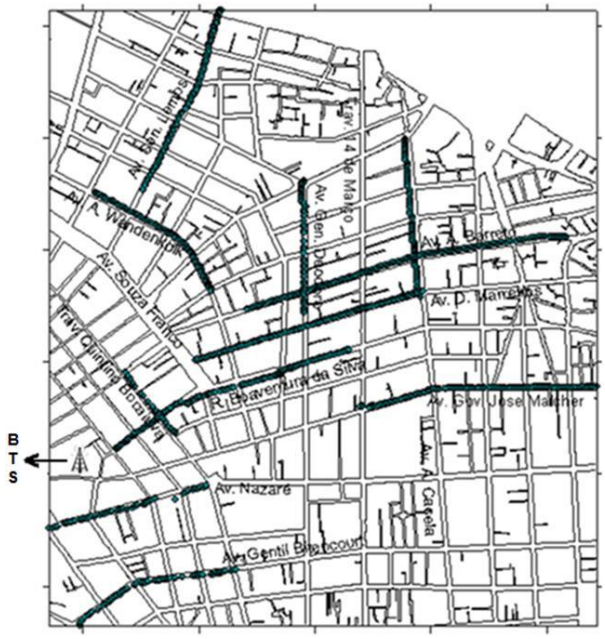

Fig. 3: Sampling points for power measurement in the study area [5]

5.2 Methodology

5.2.1 Analysis in Time Series

For the statistical analysis of received power along the pathways under study, was used time series model with the use of transfer function for modeling multivariate data sets of received power primarily along the eleven previously mentioned pathways, considering as the response variable and the received power variable distance between the transmitter and receiver, the distance between the height of buildings and buildings as covariates. All analyzes were performed using programs developed with the routines of the statistical soft SAS(*SAS/ETS 9.1 User's Guide*, 2004) [28], which through the subroutine proc arima held the adjustment of ARIMA models. This adjustment, which is performed iteratively, consists of three steps. The first is the identification of the model, where the observed data is transformed into a stationary series. The second step is to estimate the model in which the orders p and q are selected, and the corresponding parameters estimated. The third step is the prediction, in which the estimated model is used to predict future values of the time series considered.

The Figs. 4 to 6 present the graphs of the series which will be analyzed with data collected in eleven ways of the measuring campaign.

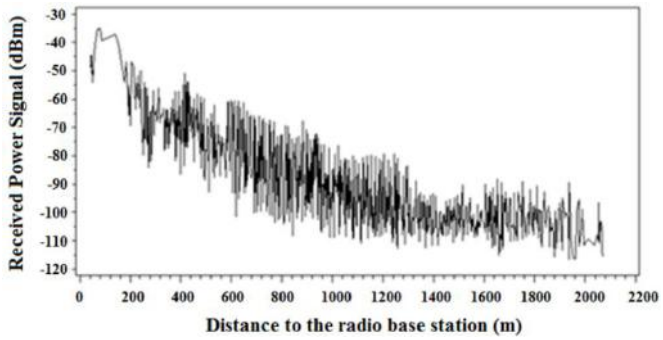

Fig 4: Receivedpowersignal (dBm)

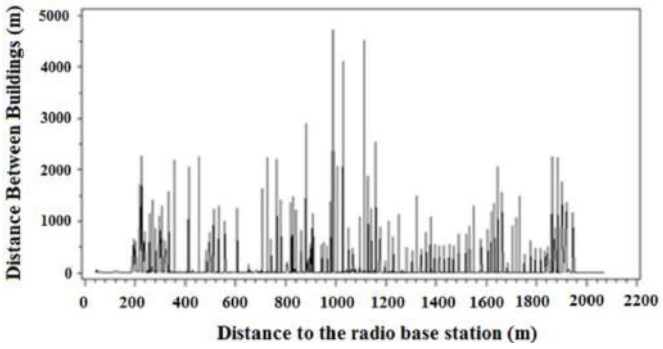

Fig 5: Distance between buildings (m)

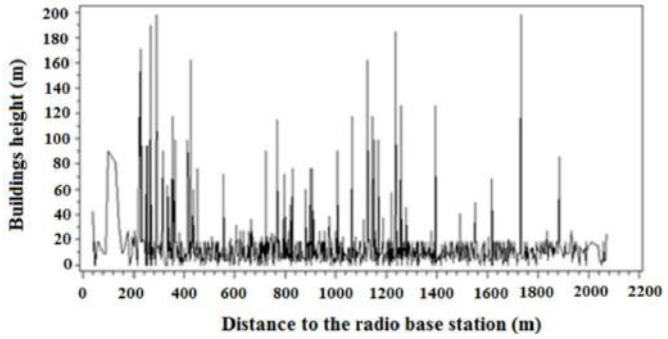

Fig: 6: Height of the buildings (m)

5.2.1.1. Adjustment of Univariate Models for the Explanatory Variables - Identification of Time Series

This phase consists in determining which process generating the series, which filters (ARIMA models) and their orders. The completion of the identification process, in addition to graphical analysis, needs in general the interpretations of the autocorrelation function and partial autocorrelation function. In this study, the identification of each series was conducted using the soft SAS. For the series received power was applied a difference to make it stationary. In all cases, the estimated parameters were significant autocorrelation and residues had no significant, a sign acceptable fit as shown in Table 1. As of now the response variable of received power will be denoted by Y_d and the explanatory variables distance between buildings and height of buildings by X_{1d}andX_{2d}, respectively.

From the analysis of the autocorrelations and partial autocorrelations preliminary models were adjusted for the series (p indicates the significance of the estimate); the results are shown in Table 2. In all cases, the estimated parameters were significant autocorrelations and residuals showed no significant signal adjustment acceptable for the model.

Table 1: ARIMA model adjusted to the series input.

Series (variable)	χ^2	$P_r > \chi^2$	Cross correlations					
Y_d	5.18	0.3946	-	-0.015	-0.038	-0.006	0.018	0.041
	8.37	0.6796		0.013	-0.026	-0.040	-0.023	0.015
X_{1d}	9.47	0.0916	-	-0.029	0.009	-0.045	-0.029	0.054
	13.07	0.2888		-0.017	0.046	0.004	-0.024	0.025
X_{2d}	3.13	0.9995		0.003	0.019	-0.028	-0.017	-0.044
	7.38	0.2868		0.035	-0.006	0.003	0.006	-0.002

Table 2: ARIMA model adjusted to the series input.

Series (variable)	Adjusted Model	Model
Y_d	$Y_d = Y_{d-1} - \underset{p<0,0001}{0,91}\ a_{1d-1} + a_{1d}$	Arima(0,1,1)
X_{1d}	$X_{1d} = \underset{p<0,0001}{128,58} + \underset{p<0,0151}{0,077}\ X_{1d-7} + a_{2d}$	Arima(1,0,0)
X_{2d}	$X_{2d} = \underset{p<0,001}{14,870} + \underset{p<0,0171}{0,076}\ X_{2d-2} - \underset{p<0,034}{0,068}\ X_{2d-9} - \underset{p<0,0109}{0,081}\ X_{2d-11} - \underset{p<0,047}{0,063}\ X_{2d-12} - \underset{p<0,045}{0,064}\ X_{2d-14} - \underset{p<0,038}{0,066}\ X_{2d-15} + a_{3d}$	Arima(6,0,0)

Where *d*: is the distance index, Y_d,X_{1d} and X_{2d} are the variables; a_{1d},a_{2d} and a_{3d} are random errors, p is p-value.

To identify the model transfer function suitable for a data set, one must consider the graph of the cross-correlation function sample. For the cross-correlation function be meaningful, the series of input and response should be pre-filtered.

For pre-filtering the series of input and response appropriate to analyze the correlation, the procedure is as follows:

1. Adjusting an ARIMA model to the series input so that the model residuals are white noise;
2. Filter the host response to the same template used to input the serial:;
3. Making the cross-correlation of the series of filtered response to the filtered input string to determine the relationship between the series;
4. Interpret the cross-correlation graph in the same way a graph of the autocorrelation function. Indicators autoregressive *s* terms indicate the denominator and indicators moving averages indicate terms of the numerator.

The graph of cross correlation pre-filtered with a transfer function numerator terms q and p in accordance with the denominator shows the same pattern after *slags*, such as the graph of the autocorrelation function of an ARMA process (p,q). This is the key to identify the transfer function. Such behavior is not guaranteed without pre-filtering, however. The ARIMA procedure automatically makes the pre-filtering when including the appropriate declarations in code soft SAS [28].

The adjusted model for the received signal power (Y_d) includes explanatory variables X_{1d} (Distance between buildings) and X_{2d}(Height of building) and, according to

the analysis of cross correlations and after a few attempts, the following transfer function model was specified:

$$Y_d = \frac{w_0 + w_2 B^2}{(1-\delta_1 B - \delta_9 B^9)} X_{1d} + \frac{w_0}{(1+\delta_1 B)} X_{2d-1} + N_d \quad (34)$$

The Tables 3 and 4 show estimates of the model parameters of the transfer function obtained through a program of soft SAS and residual analysis for the model obtained, respectively. It is observed that statistics of cross-correlations with the waste input variable were not significant, i.e, the model transfer function provides a proper fit to the data. All parameters showed significant estimates, but the check of residual autocorrelations shows significant value in *lag* 1 (in bold) as shown in Table 4, this indicates that the residuals of this preliminary model are not white noises. That is, it is necessary to estimate parameters for the error process (N_d) for this model.

Table 3: Estimates and statistics of transfer function model obtained by iterative (SAS)

Parameter	Estimate	t value	$P_r > \|t\|$	Lag	Variable
Numerator 1	-	-8.08	<.0001	0	X_{1d}
Numerator (1,1)	-	-2.61	0.0090	2	X_{1d}
Denominator (1,1)	-0.77979	-7.52	<.0001	1	X_{1d}
Denominator (1,2)	0.12130	2.69	0.0071	9	X_{1d}
Numerator 2	0.02997	2.51	0.0121	0	X_{2d}
Denominator (2,1)	-0.78529	-6.20	<.0001	1	X_{2d}

Table 4: Residual analysis for the model

Until the	χ^2	$P_r > \chi^2$	Cross correlations					
6	240.31	<.0001	**-0.498**	0.006	-0.024	0.003	0.014	0.028
12	245.96	<.0001	-0.046	0.029	0.012	-0.048	0.020	0.007
18	248.38	<.0001	0.009	-0.006	-0.025	0.034	-0.016	0.017
24	264.80	<.0001	0.027	-0.044	-0.028	0.067	-0.063	0.068

The equation of the model in notation B of a delay operator can be written as:

$$Y_d = \frac{-0.0055 + 0.00287B^2}{(1 + 0.7799B - 0.1213B^9)} X_{1d} - \frac{0.0299}{(1 + 0.78529B)} X_{2d-1} + N_d \quad (35)$$

The Figs. 7 and 8 show the autocorrelation function (ACF) and a Partial autocorrelation function (PACF) for the residuals. It is clearly observed a high correlation value for *lag* 1 in Fig. 7, evidencing a high correlation between the residuals. This residual analysis can indicate possible missing terms in the model.

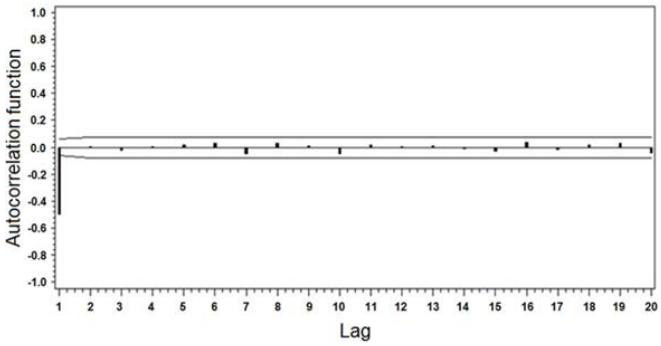

Fig. 7: Analysis for autocorrelation functions (ACF) of residuals (N_d)

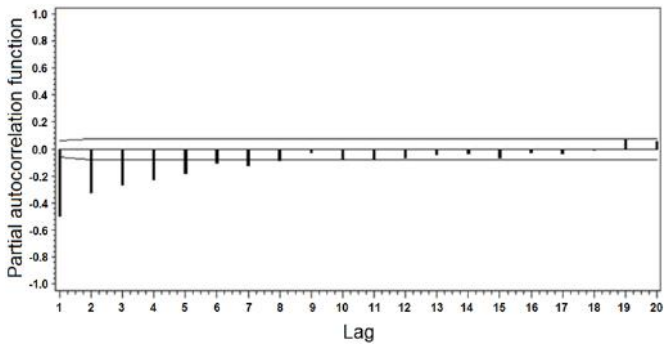

Fig: 8: Analysis for partial autocorrelation functions (PACF) of residuals (N_d)

5.2.2. Geostatistical analysis

In the previous section, we estimated a model in time series with transfer function models in which the residues (N_d) these models are not white noise.

Note that the adjusted model was considered only the macro-localized features existing in the data of the residue of the received signal power, calculated by the time series model, it is not yet taken into account the influence that the data have on its neighbors, the small spatial scale. In other words, the residuals of this model are still present in two components: *ε'(x)+ε"*, is only ε" is distributed independently. In this case, the estimated residuals may still be contaminated by the effect of spatial dependence on small spatial scale.(Fischer & Nijkamp, 1992) [29].

5.2.2.1. Spatial Autocorrelation Diagnosis

One of the ways to diagnose the presence of spatial effects in the data of the residue of the time series model is previously calculated by graphical analysis of the experimental semivariogram. The spatial inference is performed by kriging process which is based on the Regionalized Variable Theory (RVT). This theory identifies the spatial distribution of a variable is expressed by the sum of three components: one structural component having a constant mean or trend; one spatially correlated random component, also called regionalized variation; one spatially uncorrelated random component (residual error).

The analysis of spatial variability of residuals in time series models, calculated by the equation, is carried out with the aid of a semivariogram. This is one of the most important steps of the geostatistical analysis, because the semivariogram model chosen represents the spatial correlation structure to be used in inferential procedures of kriging. The results presented in Fig. 9 shows the omnidirectional semivariogram (isotropic case) and its adjustment model.

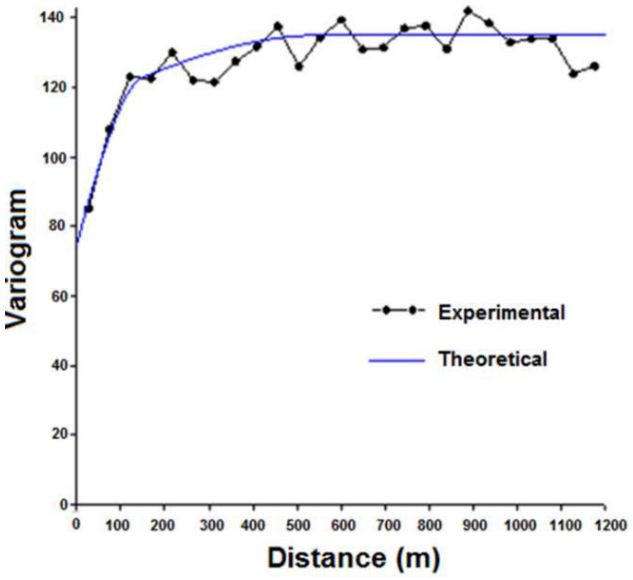

Fig 9: Experimental variogram and theoretical of residues

Whose parameters are the equation 36, is the nested type (double spherical), that is, a combination of two spherical models.

$$\gamma(h) = 75 + 40\left(\frac{150}{2h} - 1{,}5\left(\frac{150}{h}\right)^3\right) + 20\left(\frac{500}{2h} - 1{,}5\left(\frac{500}{h}\right)^3\right) \quad (36)$$

where:

a_1 = 150 *and*C_1 = 40 correspond to the range of parameters and input, respectively, of the first spherical model ($\gamma_{1(h)}$).

a_2 =20 andC_2 = 500 correspond to the range of parameters and input, respectively, of the second spherical model ($\gamma_{2(h)}$).

Based on the structure defined as nested semivariogram (double spherical was performed a spatial inference spatial the kriging process, obtaining the map of the spatial distribution of power received through the program SURFER(Al-sudani, 2019; Bresnahan & Dickenson, n.d.) [30-31].

With equation 50 establishes the geostatistical modeling of residual (N_d) acquired by the time series model (equation 35). The model establishing calculating of the received power in the searched area is given by:

$$Y_d = 75 + \frac{-0{,}0055 + 0{,}00287B^2}{(1 + 0{,}7799B - 0{,}1213B^9)}X_{1d} - \frac{0{,}0299}{(1 + 0{,}78529B)}X_{2d-1} + 40\left(\frac{150}{2h} - 1{,}5\left(\frac{150}{h}\right)^3\right) + 20\left(\frac{500}{2h} - 1{,}5\left(\frac{500}{h}\right)^3\right) + e_d \quad (37)$$

where h is given in meters,

e_d: random error.

Analyzing autocorrelation functions and partial autocorrelation of the residues model found (equation 37) of Figs. 10 and 11. One can notice a substantial decrease in the residual autocorrelation (e_d) when compared to the residues obtained from the time series model (equation 35). Note that there is a significant decrease in the value of the autocorrelation for *lag* 1 (Fig. 10) when compared with Fig. 8. Since non of the *lags* present significant *spike*, soon can be stated that the number of residues of the simulated model is stationary (e_d is a white noise).

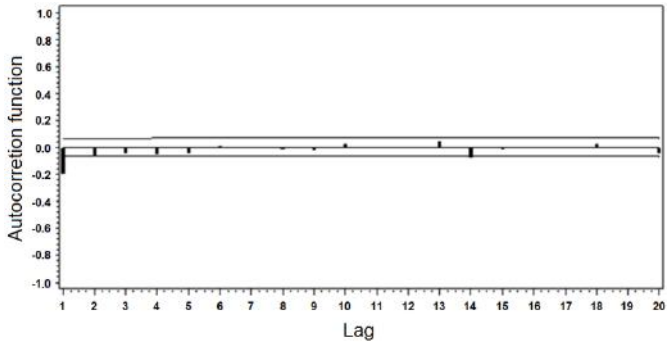

Fig 10:Analysis for autocorrelation functions (ACF) of residuals(N_d)

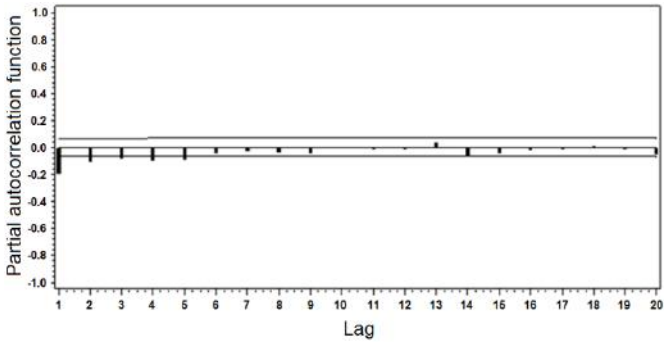

Fig 11:Analysis for partial autocorrelation functions (PACF) of residuals (N_d)

5.2.2.2. Spatial Inference with Kriging

Using the parameters of the semivariogram was held to spatial inference through the process of kriging, obtaining the spatial distribution map of the received signal power (dBm) (simulated model – equation 37) shown in Fig.12. Fig.13 shows the spatial distribution of color levels which provides information on the pattern of distribution of the received power (dBm) obtained in the measurement campaign. One can observe the potential of the methodology adopted, when comparing the maps indicate the spatial distribution of the received power (dBm) by the receiving unit.

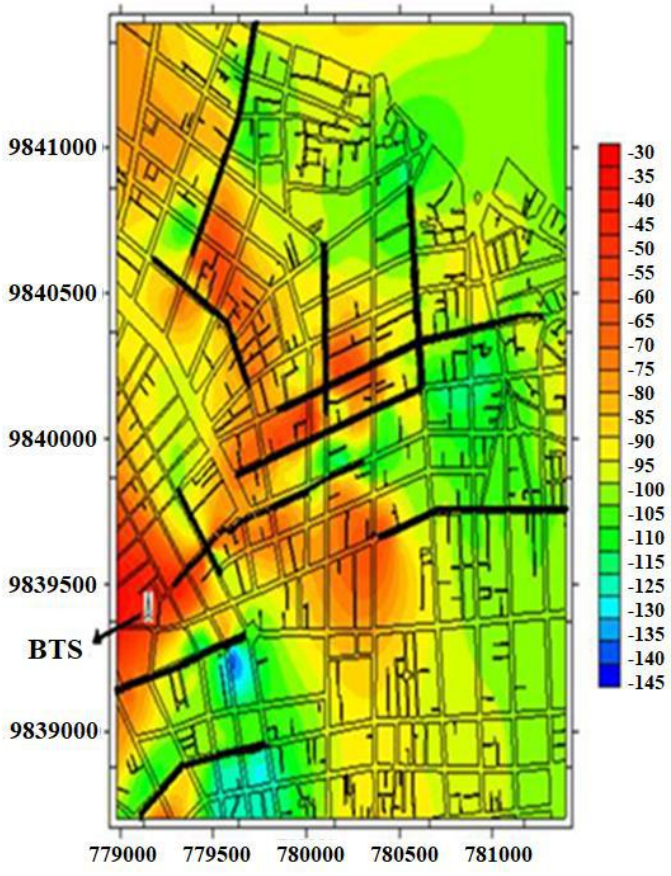

Fig 12: Spatial distribution map of received power (dBm) for Model simulated

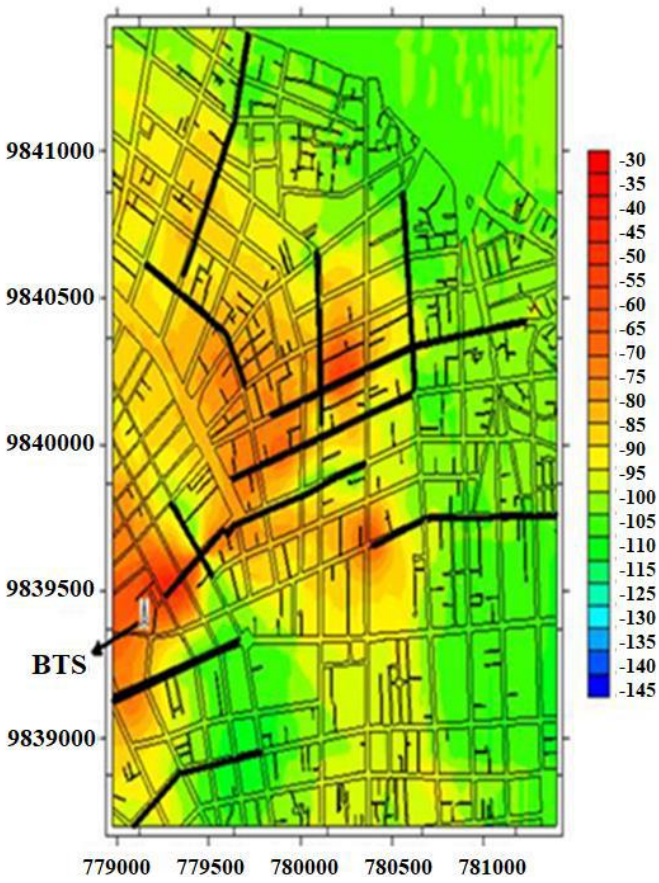

Fig 13:Spatialdistributionmapofreceivedpower (dBm) for measurementcampaign

Note that the kriging shown in Fig. 12 and 13, where one can observe the areas with greater or lesser value of receipt of received power, according to the gradient of colors that allows visual analysis faster and simpler of the study area. Note that there is some agreement between the profile displayed by the maps obtained with the predicted values with the simulated model (Fig. 12) and field data (Fig. 13).

The spatial distribution of values shows the regions marked in red as higher levels of received power (dBm). The regions in green and blue are areas with lower signal intensity. As might be expected, it is observed higher levels of power to the vicinity of the base station and other areasnot far from the BTS.

Note also that much of the region that has a low levelsignal is located at great distances from BTS, however, in the lower left corner of the maps (which are located AvenidasNazaré and Gentil Bittencourt), there is a region of low signal intensity, which can be explained by the higher incidence of heights of buildings and also with tunnels formed by mango trees present on these two pathways.

Fig. 14 the graph shows the response for the model and observed values of the response variable power received through simulated time series models with error correction using a geostatistical model. The confidence intervals of 95% are indicated by the yellow shaded area.

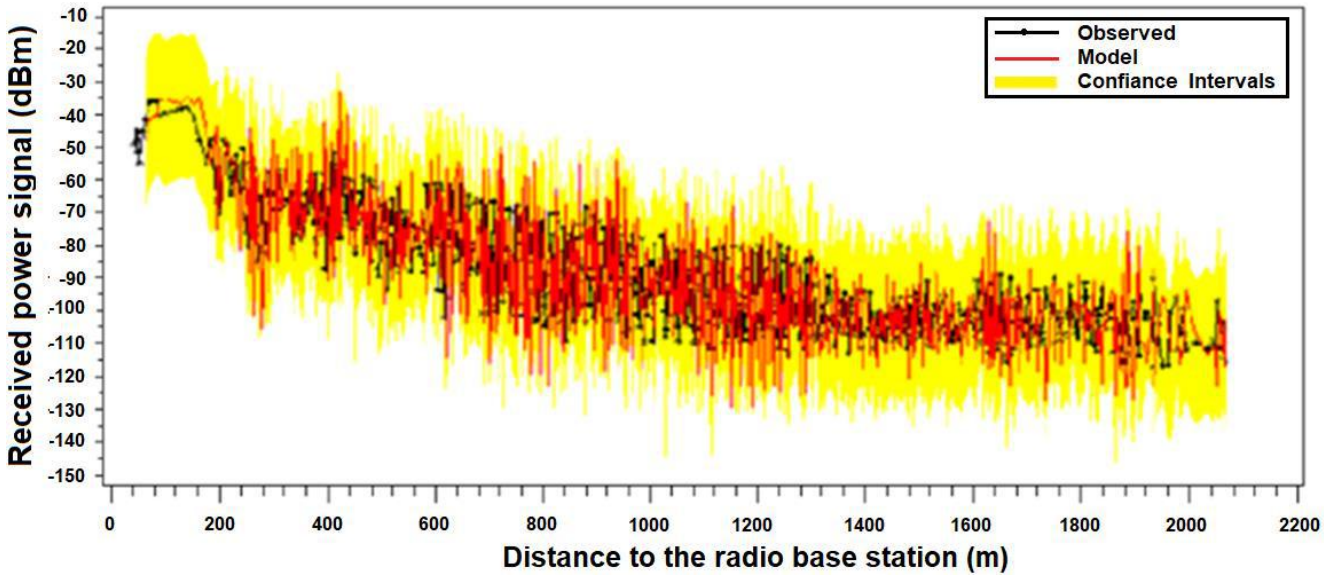

Fig 14:Power of the signal received by the mobile station and estimated by theoretical models and simulated

VI. COMPARATIVE ANALYSIS OF THE RESULTS

After conducting the comparative analysis of the results obtained in measurements with the prediction of theoretical models of Ikegami-Walfisch, Ibrahim-Parsons and Okumura-Hata and the simulated model. The theoretical models consider when calculating the signal attenuation parameters such as height of the transmitting antennas of receptor, types of cities, the average height of the buildings, width of streets, operating frequency and types of urbanization (rural suburban and urban), and the dependence on the distance.

The parameters used in the analysis of models had the following values: The receiving antenna height: $h_r = 15\,m$; the receiving antenna height: $h_t = 35\,m$; the operating frequency: $f = 877.44$ MHz and average width of the street: $W = 22\,m$.

For the qualitative analysis of the measures with forecasts. In Figure 15 we present the experimental results and theoretical simulations performed by the models of Ibrahim-Parsons and Okumura-Hataand the response of the

simulated model time series with error correction developed in this work, to eleven routes from the center of the city of Belém/PA. Table 5 presents the values of the mean square error, the mean and standard deviation.

Table 5: Comparison between the three theoretical models and the measured value for the pathways involved in the measurement campaign

	Mean Squared	**Mean (dBm)**	**Standard Deviation**
Measured	-	-89.7875	15.7682
Proposed	0.33	-89.6232	18.0632
Ikegami-	39.79	-	9.6217
Ibrahim-	13.26	-79.8502	11.0363
Okumura-Hata	16.56	-76.2557	8.8080

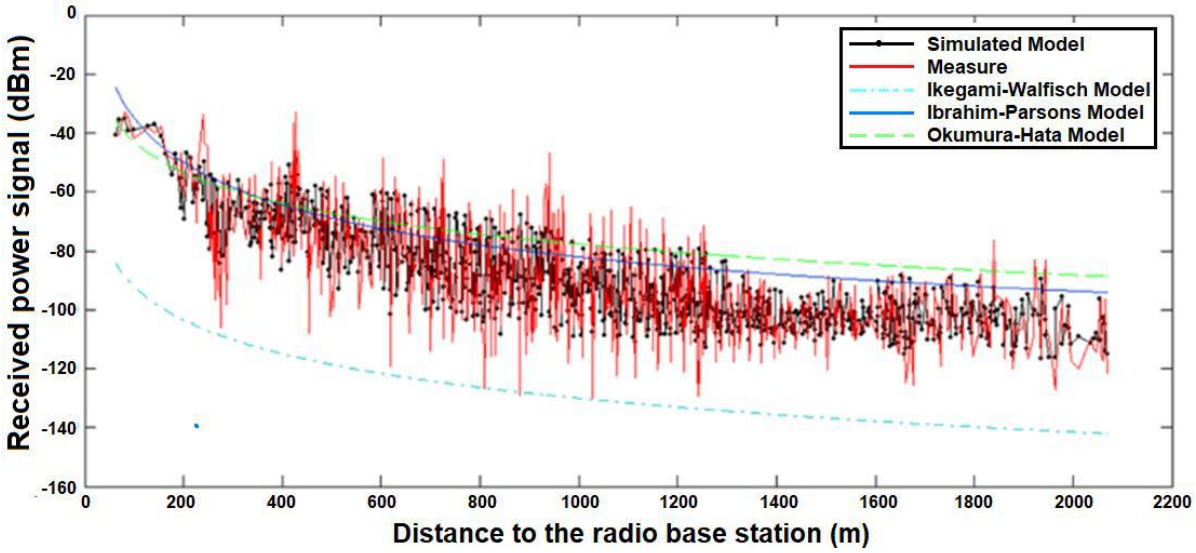

Fig. 15: Power of the signal received by the mobile station and estimated by theoretical models and simulated

Observing Table 5, it is found that, among the models given above, what best describes the signal in the study area is the simulated model developed in series with error correction using geostatistics, which presented an root mean square error 0.33 dB and the standard deviation 18.0632. However, between theoretical models, which is closer to the measurements of the model of Ibrahim-Parsons which showed a root mean square error of 13:26 dB and the standard deviation 11.0363. The model of Okumura-Hata presented the worst results.

In order to make a study of the performance of the proposed model, in order to check its validity, analysis was performed using data collected in another way of measuring campaign (RuaConselheiro Furtado), which was not part of the data processing for obtaining the coefficients entered into the equation (37). Table 6 shows the results of experimental simulations performed by the theoretical model of Ikegami-Walfisch, Ibrahim-Parsons and Okumura-Hataand the response of the simulated model obtained for the RuaConselheiro Furtado.Fig. 16 shows the comparative graph of received signal strength versus distance from the base station to RuaConselheiro Furtado.

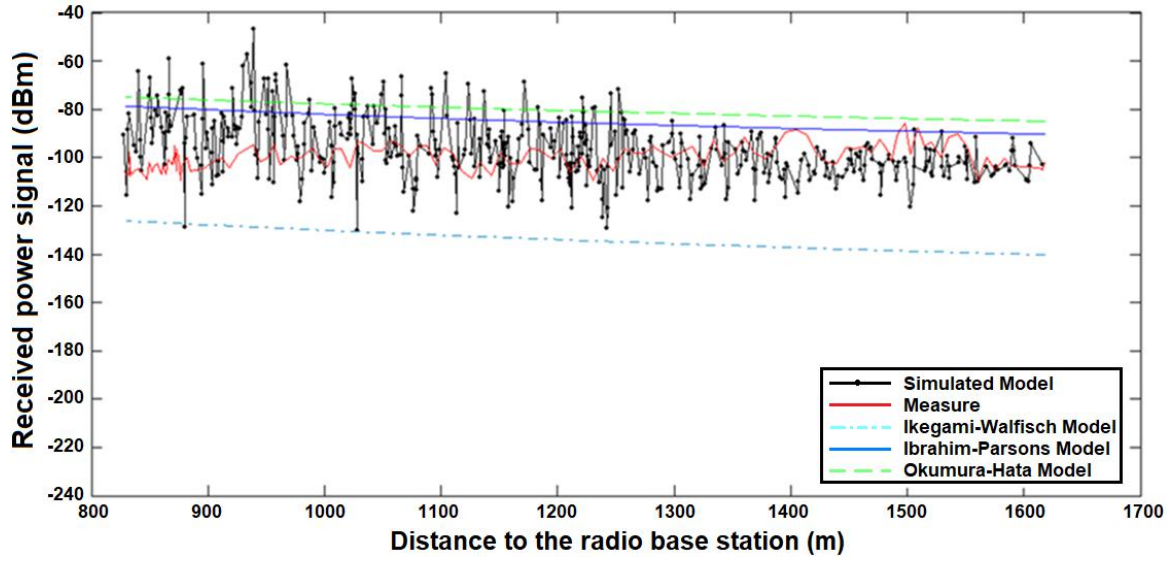

Fig 16: Power ofthesignalreceivedbythe mobile stationandestimatedbytheoretical models andsimulated for Rua Conselheiro Furtado.

Table 6: Comparison between the results obtained for the three theoretical models, simulated model and the measured value for RuaConselheiro Furtado

	Mean Squared	Mean (dBm)	Standard Deviation
Measured	-	-99.4415	9.0356
Proposed	9.04	-	12.8125
Ikegami-	37.73	-	3.8444
Ibrahim-	14.24	-	3.1487
Okumura-Hata	18.40	-	2.7320

VII. CONCLUSIONS

In this work was presented a time series model with error-correlation through geostatic, which consist a forecast of received power along the eleven pathways localized in the urban center of the city of Belém/PA. There has been shown a study of possible relationships existing between the received power signal, the height of buildings, and also the distance between the buildings. Transfer function models have been used for assessment of the received power signal in time series. As the models of classical statistical ignore the possible correlations between neighboring samples, not exploring in a satisfactory manner, the relationships that may exist between the sampling units. The error correction model time series was performed using a geostatistical model that considered the georeferencing data, which allowed the identification of these interaction effects in the same space, using kriging process.

The proposed model showed a good result with mean square error in the order 0.33 dB compared to the measured signal, considering the data of the eleven ways of the measurement campaign; while for models of Ibrahim Parsons and Okumura-Hata this error was around 13:26 and 16:56 dB, respectively.

The results show that the adjusted models retained the same characteristics of the original signal. Moreover, this methodology allows for individualized assessment of all points in the region considered, from the knowledge of their geographical coordinates, and not only the demonstration of generic values as occurs in traditional preparation of propagation models Thus, we obtained estimates of statistics, graphs and maps of dispersion and surface to describe the behavior of spatially variable received signal strength (dBm) in the center of the city of Belém/Pa.

Therefore, the study conducted through statistical analysis in time series with transfer function models and the study of spatial variability of the variables of interest allowed the construction of a model that allowed us to identify by the spatial plant the measurements of received power (dBm) and the gradient of the lines of iso-values, the vectors for better signal reception issued by BTS, identifying homogeneous areas, as well as those where users are harmed or benefited from the service of the local operator.

ACKNOWLEDGEMENTS

The authors thank the Capes and Project Ericsson/Oi Celular/UFPA for the experimental setup and the data used.

REFERENCES

[1] Liaskos, C., Nie, S., Tsioliaridou, A., Pitsillides, A., Ioannidis, S., & Akyildiz, I. (2018). A New Wireless Communication Paradigm through Software-Controlled Metasurfaces. *IEEE Communications Magazine*, *56*(9), 162–169. https://doi.org/10.1109/MCOM.2018.1700659

[2] Salous, S. (2013). *Measurement and Channel Modelling Radio Propagation Measurement and Channel Modelling*. John Wiley & Sons Ltd.

[3] Sun, Shu, Rappaport, T. S., Heath, R. W., Nix, A., & Rangan, S. (2014). MIMO for millimeter-wave wireless communications: Beamforming, spatial multiplexing, or both? *IEEE Communications Magazine*, *52*(12), 110–121. https://doi.org/10.1109/MCOM.2014.6979962

[4] Arthur, J. K., Amartey, A. T., & Brown-Acquaye, W. (2019). Adaptation of the Okumura-Hata Model to the Environment of Accra. *2019 International Conference on Communications, Signal Processing and Networks, ICCSPN 2019*, 1–6. https://doi.org/10.1109/ICCSPN46366.2019.9150198

[5] Rozal, E., Pelaes, E., Queiroz, J., & Salame, C. (2012). Modeling of wireless networks using multivariate time models. *Eurasip Journal on Advances in Signal Processing*, *2012*(1), 1–13.https://doi.org/10.1186/1687-6180-2012-248

[6] Alqudah, Y. A. (2013). On the performance of Cost 231 Walfisch Ikegami model in deployed 3.5 GHz network. *2013 The International Conference on Technological Advances in Electrical, Electronics and Computer Engineering, TAEECE 2013*, 524–527. https://doi.org/10.1109/TAEECE.2013.6557329

[7] Konak, A. (2010). Estimating path loss in wireless local area networks using ordinary kriging. *Proceedings - Winter Simulation Conference, Badman 2006*, 2888–2896. https://doi.org/10.1109/WSC.2010.5678983

[8] Phillips, C., Ton, M., Sicker, D., & Grunwald, D. (2012). Practical radio environment mapping with geostatistics. *2012 IEEE International Symposium on Dynamic Spectrum Access Networks, DYSPAN 2012*, 422–433. https://doi.org/10.1109/DYSPAN.2012.6478166

[9] Kolyaie, S., Yaghooti, M., & Majidi, G. (2011). Analysis and simulation of wireless signal propagation. *Archives of Photogrammetry, Cartography and Remote Sensing*, *22*(1), 261–270.

[10] Zhang, Y., Hamm, N. A. S., Meratnia, N., Stein, A., van de Voort, M., & Havinga, P. J. M. (2012). Statistics-based outlier detection for wireless sensor networks. *International Journal of Geographical Information Science*, *26*(8), 1373–1392. https://doi.org/10.1080/13658816.2012.654493

[11] Karunathilake, A., A. P. Chamikara, M., & Gunatilake, J. (2014). Web GIS to Identify the Problematic Mobile Signal Clusters. *International Journal of Computer Applications*, *88*(10), 30–34. https://doi.org/10.5120/15390-3832

[12] Molinari, M., Fida, M. R., Marina, M. K., & Pescape, A. (2015). Spatial interpolation based cellular coverage prediction with crowdsourced measurements. *C2B(I)D 2015 - Proceedings of the 2015 ACM SIGCOMM Workshop on Crowdsourcing and Crowdsharing of Big (Internet) Data, Part of SIGCOMM 2015*, 33–38. https://doi.org/10.1145/2787394.2787395

[13] Wen-jing, L., Chen, C., Peng, Y., & Ao, X. (2017). Traffic Prediction for Wireless Communication Networks Using S-ARIMA Model. *Journal Of Beijing University Of Posts And Telecom*, *6495*(9), 32–42.

[14] Zhang, K., Chuai, G., Gao, W., Liu, X., Maimaiti, S., & Si, Z. (2019). A new method for traffic forecasting in urban wireless communication network. *Eurasip Journal on Wireless Communications and Networking*, *2019*(1). https://doi.org/10.1186/s13638-019-1392-6

[15] Mezhoud, N., Oussalah, M., Zaatri, A., & Hammoudi, Z. (2020). Hybrid Kriging and multilayer perceptron neural network technique for coverage prediction in cellular networks. *International Journal of Parallel, Emergent and Distributed Systems*, *35*(6), 682–706. https://doi.org/10.1080/17445760.2020.1805609

[16] Song, H., Sui, S., Han, Q., Zhang, H., & Yang, Z. (2020). Autoregressive integrated moving average model–based secure data aggregation for wireless sensor networks. *International Journal of Distributed Sensor Networks*, *16*(3). https://doi.org/10.1177/1550147720912958

[17] Faruk, N., Popoola, S. I., Surajudeen-Bakinde, N. T., Oloyede, A. A., Abdulkarim, A., Olawoyin, L. A., Ali, M., Calafate, C. T., & Atayero, A. A. (2019). Path Loss Predictions in the VHF and UHF Bands within Urban Environments: Experimental Investigation of Empirical, Heuristics and Geospatial Models. *IEEE Access*, *7*, 77293–77307. https://doi.org/10.1109/ACCESS.2019.2921411

[18] Sato, K., Suto, K., Inage, K., Adachi, K., & Fujii, T. (2021). Space-frequency-interpolated radio map. *IEEE Transactions on Vehicular Technology*, *70*(1), 714–725. https://doi.org/10.1109/TVT.2021.3049894

[19] Chilès, J.-P., & Delfiner, P. (2012). *Geostatistics: Modeling Spatial Uncertainty* (2nd ed., Vol. 148). John Wiley & Sons, Inc.

[20] Gooverts, P. (1984). Geostatistics for Natural Resources Characterization. In *Geostatistics for Natural Resources Characterization*. https://doi.org/10.1007/978-94-009-3701-7

[21] Isaaks, E. H. (1990). Applied geostatistics. *Choice Reviews Online*, *28*(01), 28-0304-28–0304. https://doi.org/10.5860/choice.28-0304

[22] Johnston, K., Ver Hoef, J. M., Krivoruchko, K., Lucas, N., & Magri, A. (2001). *ArcGIS 9 Geostatistical Analyst Tutorial*.

[23] PYRCZ, M. J., & DEUTSCH, C. V. (2014). *GEOSTATISTICAL RESERVOIR MODELING* (2nd ed., Vol. 148). Oxford University Press.

[24] Sun, Shiquan, Zhu, J., & Zhou, X. (2020). Statistical analysis of spatial expression patterns for spatially resolved transcriptomic studies. *Nature Methods*, *17*(2), 193–200. https://doi.org/10.1038/s41592-019-0701-7

[25] Tobler, W. R. (1989). Frame independent spatial analysis. *The Accuracy of Spatial Databases*, *December*, 115–122. https://doi.org/10.1201/b12612-33

[26] Christakos, G. (1984). On the Problem of Permissible Covariance and Variogram Models. *Water Resources Research*, *20*(2), 251–265. https://doi.org/10.1029/WR020i002p00251

[27] D. Istok, J., & A. Rautman, C. (1996). *Probabilistic Assessment of Ground-Water Contamination: 2. Results of Case Study*. https://doi.org/https://doi.org/10.1111/j.1745-6584.1996.tb02171.x

[28] *SAS/ETS 9.1 User's Guide*. (2004). 2004, SAS Institute Inc., Cary, NC, USA. http://www.ncbi.nlm.nih.gov/pubmed/4248169

[29] Fischer, M. M., & Nijkamp, P. (1992). Geographic information systems and spatial analysis. *The Annals of Regional Science*, *26*(1), 3–17. https://doi.org/10.1007/BF01581477

[30] Al-sudani, H. (2019). *Introduction to Surfer: Preliminary Training Course in Surfer Application in Contouring Mapping*. *March*. https://doi.org/10.13140/RG.2.2.33827.50729

[31] Bresnahan, T., & Dickenson, K. (n.d.). *Surfer 8 - Training Guide*.